Evidence for fire fountaining at Skillion Hill, Southern Tasmania

Author: G. Cumming, K. Orth, R. Bottrill, J. Everard, and M. Vicary

Date: 01/08/2024

Email: info@mrt.tas.gov.au

Website: www.mrt.tas.gov.au

REPORT No.:TR45

Geological Survey Technical Report 45

Tasmanian Government

Geological Survey Technical Report 45:

Evidence for fire fountaining at Skillion Hill, Southern Tasmania

by

G. Cumming, K. Orth, R. Bottrill, J. Everard, and M. Vicary

Cover: Cuspate-vesicular basalt with cryptic-clastic texture above monomictic blocky scoria-rich breccia, Skillion Hill (Photo – G. Cumming).

Abstract

At Skillion Hill, Southern Tasmania, a Cenozoic alkaline basaltic volcanic centre, 600 m in diameter, is composed of overlapping lenses of vesicular lava, fluidal and blocky basaltic breccia and dykes. Exposures of basalt with a cryptic clastic appearance occurs in contact with the breccia deposits. The cryptic-clastic texture comprises a fine network of thin, wispy-lenticular cuspate vesicles (< 0.1 mm thick) and spaced discontinuous jointing. The orientation of the vesicles conforms to the stratification observed in the scoria deposits above and below. The cuspate-vesicular basalt is locally xenolith-rich, containing hornfelsed clasts of underlying siliceous sedimentary rocks and dolerite, plus enstatite xenocrysts. Structural measurements of dykes, flow banding and the stratification in the scoria breccia facies, along with the incidence of interpreted volcanic bombs and possible proximal spatter piles or fountain-fed lavas, indicate formation in an inner-fountain or proximal volcanic setting. Therefore, Skillion Hill represents a partly dissected edifice of a fissure vent or scoria cone. It is likely that Skillion Hill was formed from eruptions of alkaline, low viscosity lava with high effusion and/or low eruption columns (to form coalesced spatter), alternating with eruptions having a higher volatile content and greater explosivity which formed more vesicular lava, breccias and volcanic bomb-rich deposits.

Tasmanian Government

Evidence for fire fountaining at Skillion Hill, Southern Tasmania

by G. Cumming[1], K. Orth[2], R. Bottrill[1], J. Everard[1], and M. Vicary[1]
[1]*Geological Survey Branch - Mineral Resources Tasmania*
[2]*School of Natural Sciences - University of Tasmania*

CONTENTS

FIGURES

1.0 INTRODUCTION

1.1 Regional geological setting

The Cenozoic volcanics of Eastern Australia (e.g. Johnson, 1989) form a broad band of intraplate volcanism that extends from Torres Strait to submerged continental fragments south of Tasmania (Crawford et al., 1997). The Tasmanian part of the province, which was active from at least 70 Ma (Zwingmann et al., 2004) to ~10 Ma (Fox et al., 2023), is wholly basaltic and has been reviewed recently by Sutherland et al. (2004) and Everard et al. (2014).

Although the Tasmanian volcanics are most voluminous in the northwest, numerous mostly small flows, plugs and diatremes occur in Southeast Tasmania (Sutherland, 1976 and 1977; Gulline, 1984). Skillion Hill centre is one of several small plugs, explosive vents and diatremes with associated scoriaceous lava flows and pyroclastic deposits, occurring particularly in the eastern outskirts of Hobart (Figure 1).

The pre-Cenozoic basement in this area consists of essentially flat-lying but extensively faulted Permian and Triassic shelf sedimentary units (Parmeener Supergroup) with numerous intrusions of Jurassic dolerite. At Skillion Hill, the volcanics (and locally thin poorly exposed pre-basalt sediments) rest on the Late Permian Abels Bay Formation, with a discordant dolerite intrusion -immediately to the west (Figure 1; Forsyth and Clarke, 1999).

Recent aeromagnetic data may support the inference that the vent for the volcanics lies directly beneath Skillion Hill, and has normal magnetic polarity. However, related volcanics extend for ~2 km northward up the valley of Clarence Plains Rivulet. These are not coincident with the same linear magnetic feature, but Jurassic dolerite exposures are. Outliers of basalt mapped at Clarendon Vale suggest that, prior to erosion, the volcanics may have formerly extended for up to 1.7 km to the east and northeast (Figure 1; Forsyth and Clarke, 1999).

1.2 Previous work

Edwards (1950) described a group of "fine-grained oligoclase-basalts, of rather unusual chemical composition" occurring at several localities in South-eastern Tasmania, including "about midway between Rokeby and Bellerive, adjacent to the road." It is likely that this location refers to the vicinity of Skillion Hill. He termed this group of basalts the "Rokeby Type" and provided a major element analysis from the type locality.

In 1961, Green described the petrography of "dense, dark grey, fine-grained basalt outcropping strongly as benches on the top of Rokeby (Skillion) Hill " (Green, 1961). On the eastern side of the hill, massive and scoriaceous basalt, interbedded with volcanic breccia and subordinate tuff", were described. On the basis of generally westward dips, a concealed volcanic centre was inferred to lie to the east, near the site of the original village of Rokeby.

Sutherland (1976), re-examined the area, and suggested that the eruptive centre lay under Skillion Hill. A change in dip of the interbedded lavas and pyroclastics, from west on the hillside to east at its eastern base, was interpreted to indicate backward slumping into the vent. Lavas emanating from the centre and flowing both to the north and south were inferred to have diverted Clarence Plains Rivulet eastward.

Published geological maps that include the area have been produced, with successively increasing detail, by Banks (1965), Leaman (1972) and Forsyth and Clarke (1999). Bottrill and Unwin (2018) also reported on the petrology, mineralogy and xenoliths of these rocks. Petrographic descriptions for C112290, C112292, G408825 and G408837 are documented in Bottrill and Unwin (2018) and additional samples evaluated geochemically (in this report) are included in Appendix 1.

1.3 Age

Direct evidence for the age of the Skillion Hill volcanic centre and associated basalt flows is sparse. Sub-basalt clays are mapped in places but are poorly exposed and undated. The nearest dated basalts, however, are petrologically similar rocks at Blinking Billy Point, Sandy Bay (26.5 ± 0.3 Ma, K/Ar; Sutherland and Wellman, 1986) and Pickett Hill, Kingston (29.4 ± 0.2 Ma, $^{40}Ar/^{39}Ar$ plateau; Everard et al., 2014). A similar Oligocene age is considered likely at Skillion Hill.

1.4 Local geology

Skillion Hill is a flat-topped hill at the southern edge of a 2.5 km long plateau of Cenozoic mugearite/basalt flows and basaltic breccias. The linear volcanic centre is positioned at the northern edge of a north-north-east trending line of volcanic centres that span from Droughty Hill, to the south (Forsyth and Clarke, 1999; Figure 1). The possible volcanic centres have penetrated Jurassic dolerite (Calver and Latinovic, 2002) and consist of evolved alkaline rocks, which generally occur as small plugs, explosive vents, diatremes and scoriaceous flows found elsewhere in Southern Tasmania (Everard et al., 2014; Calver and Latinovic, 2002). At Droughty Hill three small volcanic centres are documented, each consisting of basaltic lava and pyroclastics, with variations in composition. The northernmost centre consists of basaltic lava (dominantly sodic hawaiite, Tbhs; Figure 1) and pyroclastics, with rare to locally abundant xenoliths of both mantle lherzolite and dolerite. A ground magnetometer survey supported its identification as an eruptive neck (Sutherland, 1971). The nature of the other two occurrences, although both depicted as volcanic centres by Leaman (1972), is less clear. They are petrologically similar to the northern centre, and they may be related flow remnants. The central outcrop, at Droughty Hill itself, consists of sodic nepheline hawaiite to nepheline mugearite (Tbns and Tbm in Figure 1) and minor agglomerate with small lherzolite xenoliths. The southernmost centre comprises basaltic nepheline mugearite with rare nepheline benmoreite segregations (Tbnm in Figure 1) and locally interbedded pyroclastics.

QUATERNARY

- Quaternary sediments (Q).
- Alluvial gravel, sand and clay; alluvia fans (Qa, Qaf)
- Alluvium and marsh deposits (Qham).
- Colluvium (Qhc, Qhcd, Qhcl).
- Man-made depsoits (Qhmm).
- Alluvial fan and alluvial terrace deposits (Qppdw, Qppdc).
- Talus (Qpt, Qptb, Qptd, Qptp).

NEOGENE-PALEOGENE

- Cenozoic deposits (TQ).
- Plastic clay, silty clay and sandy clay with pebbly layers (TQch).
- Fluviatile and swamp deposits (TQd).
- Piedmont, alluvial fan, alluvial terrace, raised beach, lag and exhumed deposits (TQh)
- Agglomerate and tuff (Tbat).
- Basalt and basaltic lavas (Tb, Tbm, Tbnm, Tbns, Tbhs).
- ▲ Volcanic Centres

JURASSIC

- Dolerite (Jd).

PERMIAN

- Undifferentiated Permian sediments (P).
- Abels Bay Formation (Pua).
- Malbina Formation (Pum).
- Risdon Sandstone (Pur).
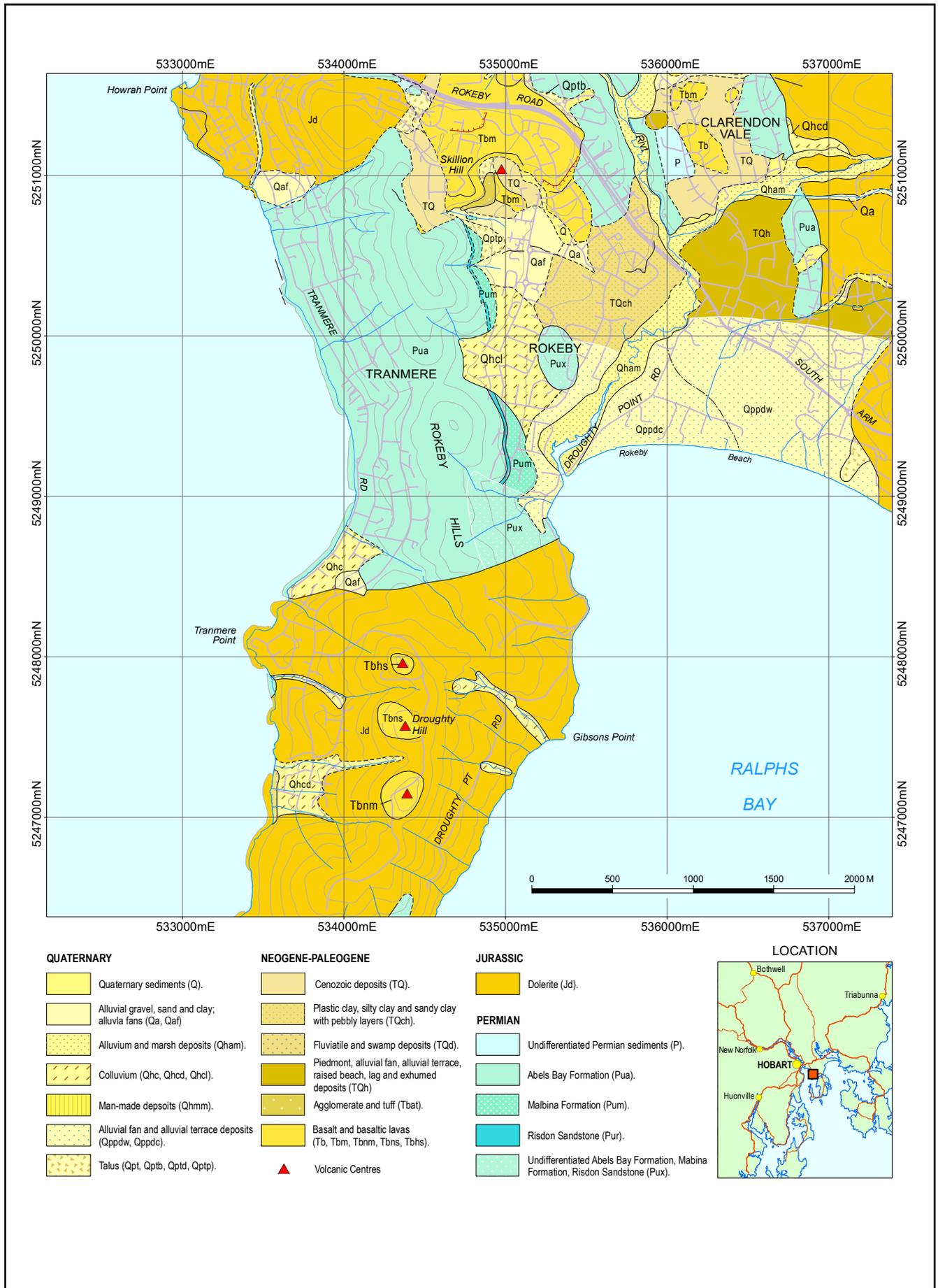- Undifferentiated Abels Bay Formation, Mabina Formation, Risdon Sandstone (Pux).

LOCATION

Figure 1. Details of 1:25 000 geological map of the area, modified from Forsyth and Clarke (1999), showing the location of volcanic centres at Droughty Hill. Note location of Skillion Hill and study area in red square.
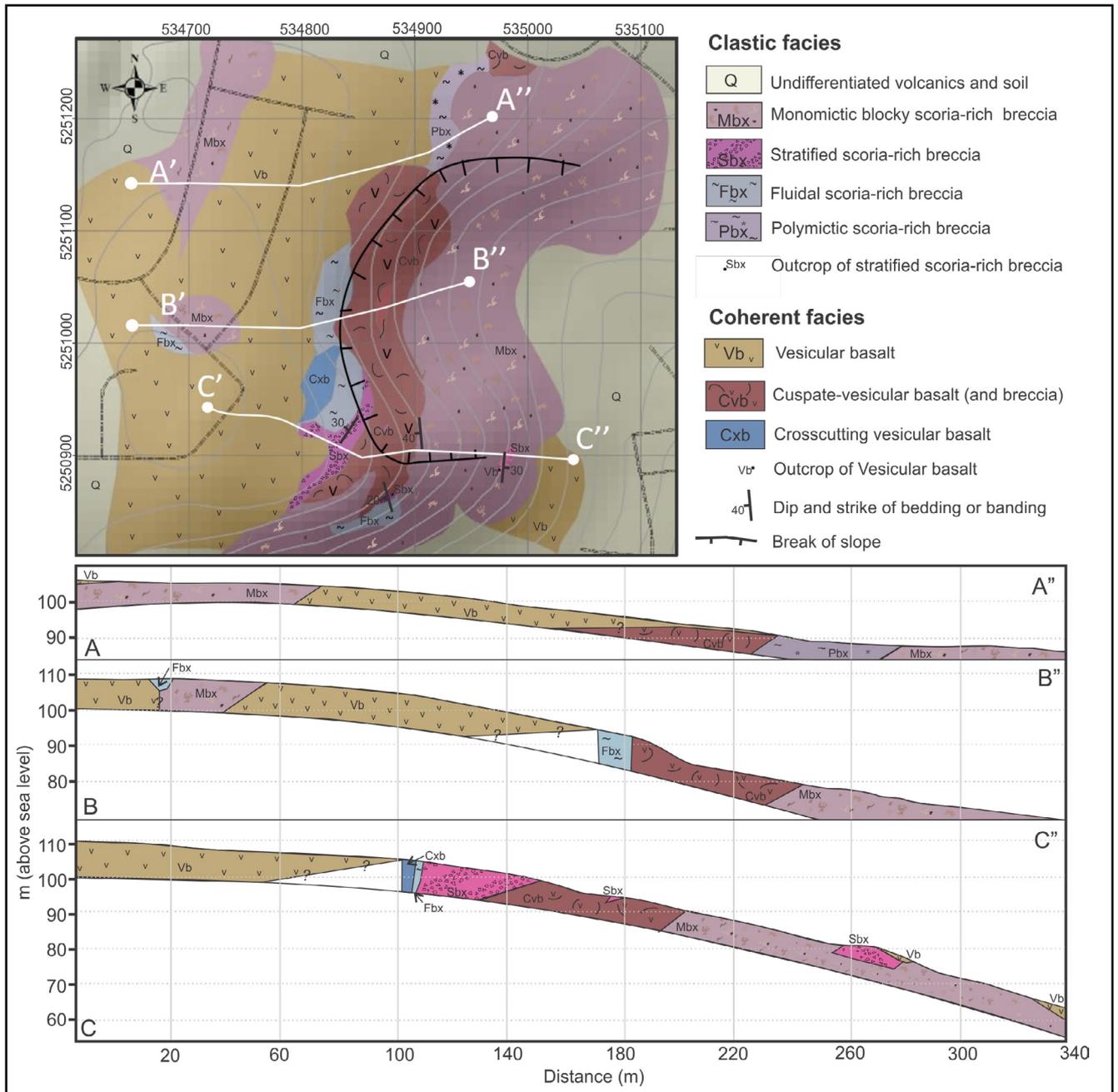
Figure 2. Geological map of Skillion Hill showing the main volcanic facies mapped, scarp and cross sections. Cross sections show attitude of cross-cutting vs. shallowly dipping facies.

The area has recently been excavated for a building subdivision, providing opportunities for sampling and re-mapping. Geological mapping traverses were conducted at Skillion Hill to understand the eruption style and architecture of the volcanics before the future housing development could obscure the exposures. The work identified diverse basaltic breccias and coherent (lava-like) facies. The area is also overlain by various Cenozoic sediments including poorly consolidated, piedmont, alluvial fan, alluvial terrace and lag deposits and Quaternary basaltic talus deposits (shown in Figure 1).

2.0 VOLCANIC FACIES AT SKILLION HILL

A simplified geological map with corresponding cross sections shows the extent of each volcanic facies (Figure 2).

Key volcanic facies include 4 breccia facies:

1. Monomictic blocky scoria-rich breccia;
2. Fluidal scoria-rich breccia;
3. Polymictic scoria-rich breccia;
4. Stratified scoria-rich breccia, and two basalt facies:
5. Vesicular basalt; and
6. Cuspate-vesicular basalt.

The characteristics of each facies is summarised in Table 1 and below.

2.1 Volaniclastic Facies

2.1.1 Monomictic blocky scoria-rich breccia

Two areas of Monomictic blocky scoria-rich breccia occur at Skillion Hill. The thickest portion forms the lower flank on the eastern side of the hill and another area of the

Table 1. Characteristics of each lithofacies subdivision observed at Skillion Hill.

Lithofacies	Description	Geometry	Key morphology or bedding characteristics
1. Monomictic blocky scoria-rich breccia	Angular to subangular basaltic clasts (80 vol%), blocky dolerite (<7 %; 1-3 cm across) and rare (< 2 %) mudstone clasts (up to 2 cm across) in a matrix of glass shards and scoria fragments (10 vol%). The clasts are dark grey to red, scoria (<80 vol%, >4 cm in diameter), sometimes with bread-crust textures and some denser basalt blocks (15 %) exhibiting minor radial polygonal joints. Dense basalt and scoria clasts typically 7 cm in diameter with a maximum size of 40 cm. Isolated zone of lobate vesicular basalt clasts (10 cm +) with irregular ragged margins (< 2 %). The matrix comprises scoria fragments and basaltic glass shards (<1 mm, 15 vol%), dark grey to brown red fresh basaltic glass shards (<1 mm, 15 vol%). Kaolinite-hematite weathered zones at higher elevation.	Tabular, continuous. At least 20 m thick.	Massive, and clast-supported. Isolated jigsaw-fit zones and transition into the poorly sorted, clast-rotated breccia.
2. Fluidal scoria-rich breccia	Monomictic elongate, vesicular, variably flow-banded (Fig. 3c), fluidal to lenticular or ribbon shaped clasts (<100%; < 0.5 cm to > 10 cm across). The clasts are dark to light grey.	Isolated lenses. Discontinuous. Less than 5 m thick.	Poorly sorted, coarse-grained, clast supported and massive. Closely associated with the cuspate-vesicular basalt.
3. Polymictic scoria-rich breccia	Abundant angular to subangular scoria (70 vol%), blocky dolerite (<15 %; 1-8 cm across) and rare (< 5 %; < 2 cm) mudstone clasts (up to 2 cm across) in a matrix of glass shards and scoria fragments (15 vol %). The basalt clasts are dark grey to brown scoria with lesser (15 %) dense basalt. Isolated zone northeast of Skillion Hill.	Lenticular? Discontinuous. Less than 5 m thick.	Poorly sorted, either clast- or matrix- supported, massive, non-stratified. Discontinuous.
4. Stratified scoria-rich breccia	Oxidised, monomictic, ragged, angular to blocky shaped vesicular basalt clasts (95 %; 1 – 10 cm). Red brown highly oxidised clasts. Some clasts are elongate (10 + %; 1 to 15 cm). The matrix consists of sand- to granule-sized, angular scoria fragments (3 %; < 0.5 cm).	Tabular-lenticular. Less than 5 m thick.	Poorly sorted, crude to moderately stratified scoria. Alternating finer grained granule rich matrix-supported layers. Clast supported coarse grained layers. Overlies cuspate-vesicular' basalt. Exhibits a westward dip ranging between 40° to 25°. Isolated (< 10 m across) lenticular zone in cuspate-vesicular' basalt.
6. Vesicular basalt/Cross-cutting vesicular basalt	Olivine basalt phenocrysts (5 % < 0.7 mm) with patchy to evenly dispersed 1-3 mm across, circular to oval vesicles and sometimes patchy close spaced < 1 mm across alteration spot textures. Angular (2 %, <5 cm) dolerite xenoliths. Monomictic, red-orange weathered blocky scoria breccia margins (clasts > 98 %; < 10 cm, no visible matrix between clasts). The outer breccia is variably weathered to an ochre-red orange colour.	Conformable and crosscutting. Tabular along the top of the hill and crosscutting neck or dyke feature beneath. Unknown thickness.	Conformable, tabular polygonal jointed basalt at higher elevation. Crosscutting basalt with brecciated margins lower down. Cross-cutting feature has north-east trending (15° to 30°) with compositional banding.
7. Cuspate-vesicular basalt	Amygdaloidal to finely vesicular (0.1 – 0.5 cm), with zeolite infilled irregular shaped ovoid to tapered, cuspate vesicles. Basalt is aphyric, fine grained (< 0.2 cm), with occasional banded texture and clastic-like appearance. < 5 cm angular to round enstatite and buchite xenocrysts (< 5 % of total volume).	Tabular-lenticular. ~10 m thick.	Massive. Orientation of arcuate lenses at the base of this zone dip 30 °east

facies occurs at the very top of the hill to the west. The breccia abuts or is overlain by Cuspate vesicular basalt on the eastern flank of the hill.

Generally, the breccia contains angular with highly vesicular scoria clasts (Figure 3a and 3b). Clasts range from cobble to boulder-size, averaging 4 cm across (but up to 40 cm across) and comprise 80 % scoria, 15 % larger (average 7 cm across) dense, very sparsely amygdaloidal basalt and blocky dolerite (<5 %; 1-3 cm across) with rare (< 2 %) mudstone clasts (up to 2 cm across). Most of the breccia is unstratified and clast-supported. Some large (up to 40 cm across) blocks of scoria have curved edges (Figure 3b) and some denser basalt blocks exhibit minor radial polygonal joints (dl in Figure 1). The breccia is red-orange in colour and weathered near the top of the hill (Figure 3a and 3b). On the eastern flank, above the 90 m elevation contour, a 2-3 m thick zone contains densely packed lobate Vesicular basalt clasts with irregular ragged margins. These clasts display moderately clast-rotated jigsaw-fit textures in places (Figure 3c). On the top of the hill, the Monomictic blocky scoria-rich breccia is highly altered with kaolinite-hematite weathered zones (Figure 3d). This area contains abundant boulder-sized scoria clasts with bread-crust textures (Figure 3e) or spindle shapes (Figure 3f) that have undergone deep weathering, resulting in a maroon-coloured, argillic soil or ferrosol.

2.1.2 Fluidal scoria-rich breccia

The Fluidal basaltic scoria breccia facies is restricted to a small zone (no more than 20 m across) near the central part of the mapped area. It has a close spatial association with the Cuspate-vesicular basalt. It shares a gradational relationship with the Monomictic blocky scoria-rich breccia (Figure 2). The facies is poorly sorted, coarse-grained, massive and generally monomictic (Figure 4), and contains elongate, vesicular, variably flow-banded (Figure 4a), fluidal to lenticular or ribbon-shaped clasts (>10 cm across). Clasts have finer grained rims suggesting possible quenched textures (Figure 6). The breccia also appears to occur along the contact of a cross-cutting basalt (dyke or apophysis) along the scarp of the hill (as depicted in Figure 2; cross sections B-B" and C-C").

2.1.3 Polymictic scoria-rich breccia

A discontinuous zone of poorly sorted Polymictic scoria-rich breccia was observed along the northeast flank of Skillion Hill. It overlies or abuts the Monomictic blocky scoria-rich breccia. These facies may share a gradational contact, although outcrops are not continuous between zones. The breccia appears to diminish towards the south, possibly beneath the Cuspate-vesicular basalt unit. The poorly sorted breccia is either clast- or matrix-supported, and contains abundant clasts of scoria, blocky or fluidal-shaped basalt, blocky dolerite, and blocky (meta?)sedimentary rocks including hornfelsed siltstone and mudstone, which may have originated from Permian facies mapped beneath. This polymictic breccia is non-stratified and is characterised by abundant angular cobble-sized dolerite clasts, comprising approximately 10-15 % of the clast components. Otherwise, it shows similar lithofacies arrangement and clast components to the Monomictic blocky scoria-rich breccia.

2.1.4 Stratified scoria-rich breccia

The Stratified scoria-rich breccia overlies and is intercalated with the Cuspate-vesicular basalt and Monomictic blocky scoria-rich breccia on the southeast flank of the Skillion Hill. It is also present as an isolated zone within the Cuspate-vesicular basalt (Figure 2; cross section C-C").

The clasts within the breccia display oxidation and have ragged, angular lenticular to blocky shapes (Figure 3b). Some clasts are elongated, ranging from 1 to 5 cm, and the matrix consists of sand- to granule-sized, angular glassy shards (Figure 5c). The stratified, scoria-rich breccia is characterised by alternating zones of crudely to moderately stratified, poorly-sorted clast-supported scoria and finer grained granule-rich, matrix-supported breccia. The stratification exhibits a westward dip ranging between 25° to 40° (Figure 2C-C"; Figure 5a and 5b). The orientation of clasts beneath an isolated zone of basalt (at 80 m elevation on cross section C-C" as shown in Figure 2) dip 30° to the east and may indicate the location where Sutherland (1976), noted a change in dip from west to east, and interpreted backward slumping into a vent under Skillion Hill.

2.2 Coherent facies

2.2.1 Vesicular basalt and Cross-cutting vesicular basalt

Tabular and cross-cutting vesicular basalt was observed at the top and low on the southeast flank of the hill (Figure 2). The tabular bodies are polygonal jointed olivine basalt with patchy to evenly dispersed vesicles and sometimes spotty texture with xenoliths (Figure 7a). Tabular Vesicular basalt overlies the Cuspate-vesicular basalt. At higher elevations, thicker (2-3 m) vesicular basalt with clast-rotated jigsaw-fit breccia is in close spatial association with the cross-cutting vesicular basalt. At the lowest point of the mapped area (at 60 m elevation) the Vesicular basalt is gradational into the monomictic basaltic breccia (Figure 7b) above. The Cross-cutting vesicular basalt (indicated in Figure 2), at the middle -southern part of the hill, neighbours a crosscutting zone of the Stratified scoria-rich breccia with fluidal clasts. In the cross-cutting body there is compositional banding trending north-east (15° to 30°). Occasionally, within the basalt, there are round to angular medium to coarse grained dolerite xenoliths measuring up to 5 cm in diameter.

Petrographically, the Vesicular basalt includes iddingsite replaced olivine phenocrysts in fine grained groundmass of tabular plagioclase and blocky clinopyroxene (Figure 7c). Vesicles are partly filled with secondary minerals such as clays? (Figure 7d). The Vesicular basalt is geochemically similar to the Cuspate-vesicular basalt (Figure 9).
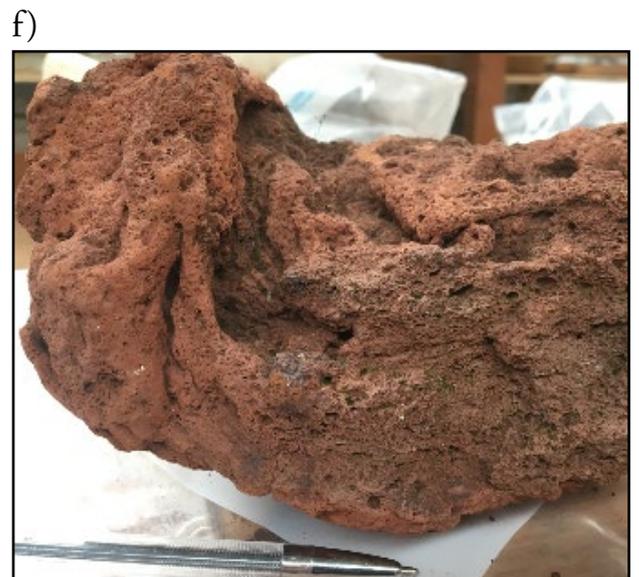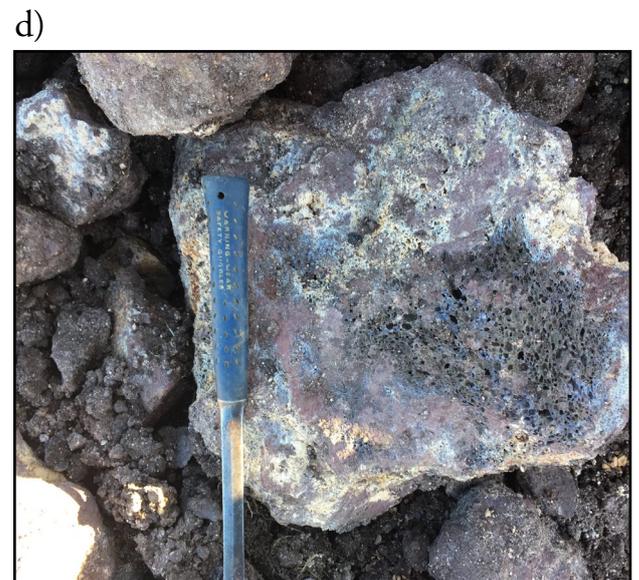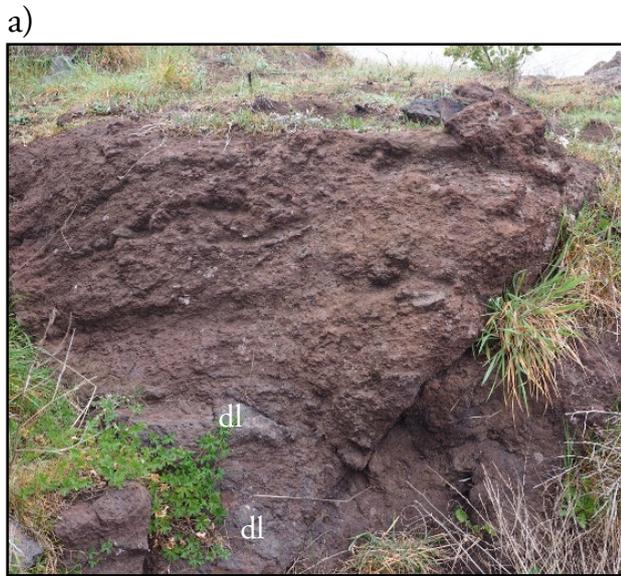
Figure 3. Monomictic blocky basaltic scoria-rich breccia. a) Breccia with angular with highly vesicular scoria clasts and basalt blocks exhibiting minor radial polygonal joints indicated as "dl" (FOV: 2.5 m) . b) Exposure with round to elongate scoria with curved edges and patchy hematite oxidation. Hand lens for scale. c) Jigsaw-fit zones in the monomictic blocky scoria breccia facies, hammer for scale. d) Highly altered scoria breccia with kaolinite-hematite weathered zones. e) Boulder-sized scoria clasts with possible bread-crust outer texture. f) Ribbon-shaped, tapered scoria with vesicular bands and breadcrust outer texture interpreted to represent a volcanic bomb scoria clast, pen for scale.
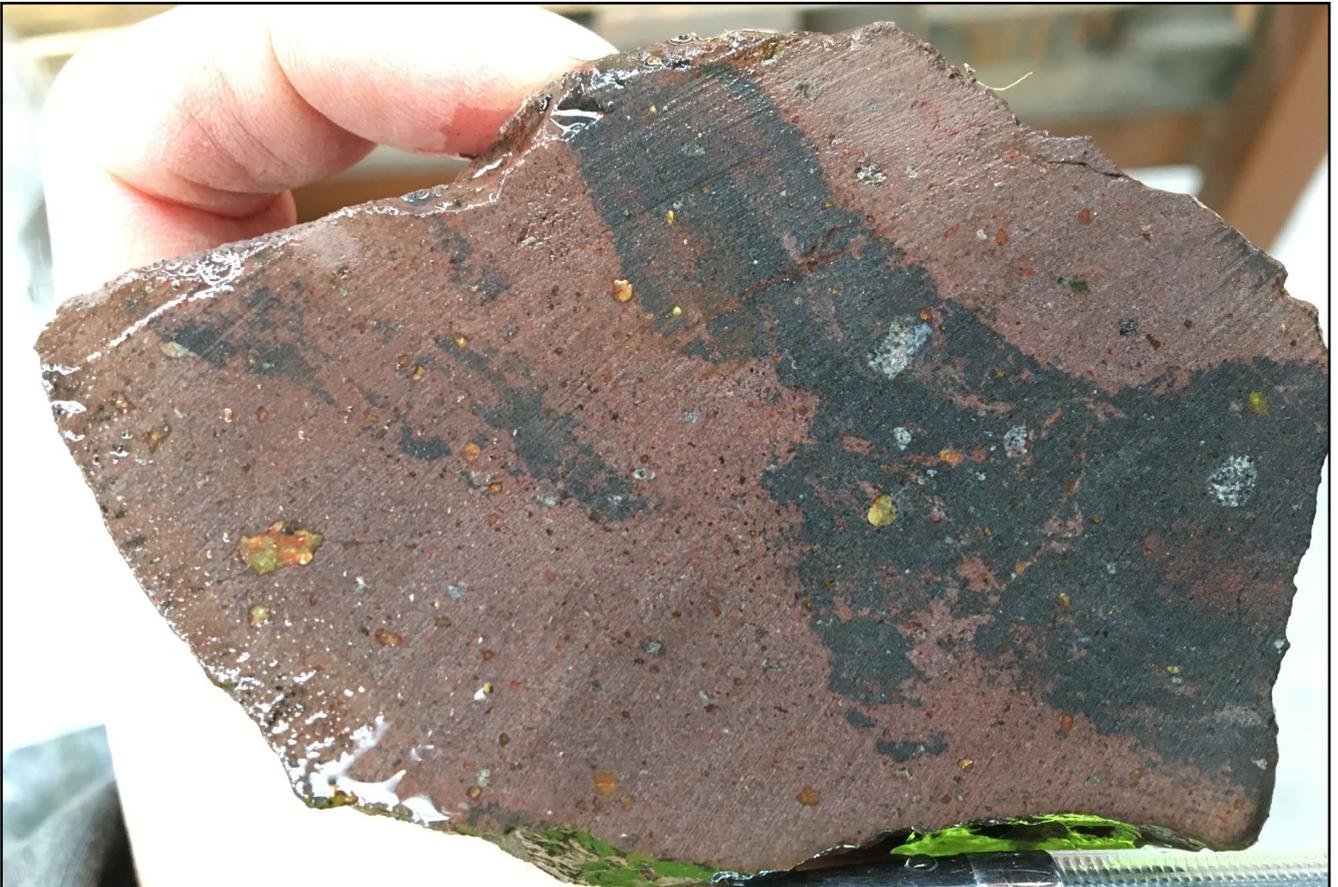
Figure 4. a) Elongate, vesicular, variably flow-banded, >10 cm long fluidal to lenticular or ribbon shaped clasts (indicated by arrow; hammer for scale) with glass shard and crystal rich matrix, and b) cut slab showing interior of fluidal clast with hematized and less altered (dark) ragged shaped unaltered ribbon shaped zones.

a)

b)
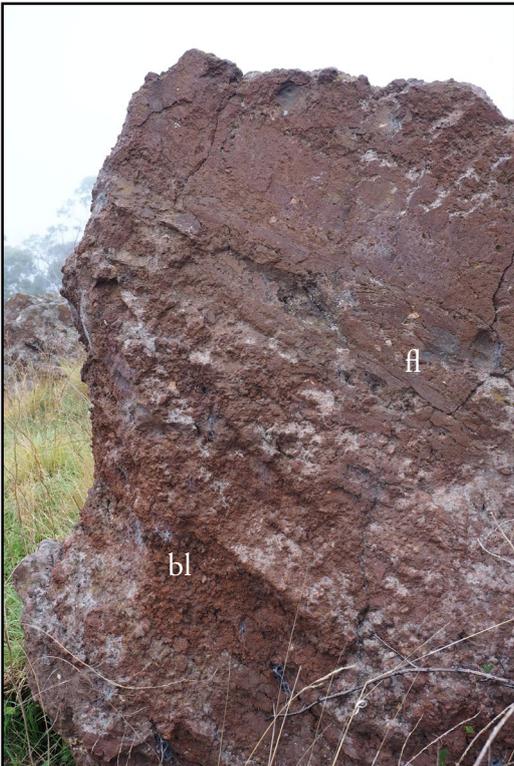
c)

Figure 5. a) Poorly sorted, crude to moderately Stratified scoria-rich breccia with alternating finer grained granule rich matrix-supported layers (shown as eroded layers). b) Oxidised, ragged, angular to blocky shaped clasts (bl) alternate with fluidal elongate clasts (fl). The matrix consists of fine grained scoria fragments. c) The clasts within the breccia display oxidation and have ragged, angular lenticular to blocky shapes ranging from 1 to 5 cm.

Figure 6. Zone of ropy, flow foliated matrix poor basaltic breccia (rbx) with irregular to fluidal margins appears gradational into vesicular basalt (vb). Hammer for scale.

2.2.2 Cuspate vesicular basalt

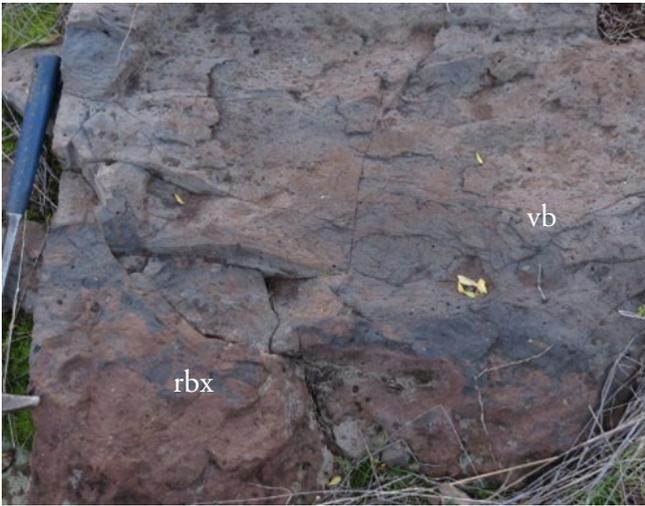A 50 m wide, ~ 300 m long lens of olivine-rich basalt with arcuate to lenticular, irregular shaped ovoid to tapered vesicles or cuspate-vesicular texture (Figure 8a) can be observed along the flank of Skillion Hill (above 90 m in elevation). The basalt overlies the Monomictic blocky scoria-rich breccia and is overlain by the Stratified scoria-rich breccia and Flow foliated (?welded) matrix-poor basaltic breccia. It is amygdaloidal to finely vesicular, with zeolite infilled, irregular-shaped ovoid to tapered vesicles. The Cuspate-vesicular basalt displays an almost clastic appearance (Figure 8b) due to a fine network of diffuse, wispy-lenticular structures (< 0.1 mm thick). The basalt displays a uniform grainsize, although a banded to platy texture is apparent throughout the central part of the unit. The base of the unit contains lenticular basalt clasts that exhibit some alignment. An isolated zone within the Cuspate-vesicular basalt contains fluidal, ribbon-like clasts (Figure 2; halfway along cross section C-C"). The wispy-lenticular structures conform to the stratification observed in the scoria deposits observed above and below. Xenoliths and xenocrysts are locally abundant (Bottrill and Unwin, 2018). These include dolerite (altered, with oxidised augite: Figure 8b), enstatite xenocrysts, and recrystallised metasedimentary clasts (anorthoclase/sanidine – aegirine-augite – tridymite – glass hornfels/buchites; Figure 8c).

The mineralogy of the Cuspate-vesicular and Vesicular basalt facies is dominated by plagioclase (oligoclase to labradorite) - augite - olivine - magnetite - ilmenite, but most olivine is now altered to iddingsite (Figure 8d and 8e), and hematite, clays (halloysite, smectite and kaolinite), and late chalcedony (Bottrill and Unwin, 2018). Hematite also occurs as a late-stage mineral and has high Ti and Mg contents. The Cuspate-vesicular basalt does not show a clastic texture in thin section (Figure 8d and 8e).

2.3 Geochemistry

Four samples from Skillion Hill were analysed for major and trace elements, using standard techniques. Two of these samples (C112290, C112292) are from the Cuspate-vesicular basalt and have weakly clastic textures, with basaltic clasts 5-10-15 mm across. Sample G408825 is a very sparsely vesicular basalt clast from the Monomictic blocky scoria-rich breccia. Sample G408837 was sampled from the Vesicular basalt. There is petrographic evidence of minor chalcedony infilling amygdales in both G408825 and G408837. Metasedimentary xenoliths occur in sample G408837.

An analysis of a sample (R010110/HBJ33) from a related flow ~1 km to the north, and the old analysis of Edwards (1950) are plotted on bivariate plots and presented in Appendix 2. None of these analyses show evidence for considerable alteration or weathering (e.g. high loss-on-ignition). However, major elements have been re-normalised to 100 % anhydrous and volatile-free, with all iron calculated as FeO. Sample locations are shown in Table 2.

Table 2. Samples analysed geochemically from the Skillion Hill area with locations.

Registration No./Field No	Lithology	mE gda94	mN gda94
C112290	Cuspate vesicular basalt	534889	5251058
C112292	Cuspate vesicular basalt	534901	5250900
G408825	Sparsely vesicular basalt clast	534749	5251244
G408837	Vesicular Basalt	534738	5251164
R010110/HBJ33	Basalt	534982	5251853
ABE6-1	Basalt	534612	5251683

All six analyses are of moderately to strongly fractionated basalts (Mg# 41.6 – 58.9). Compared to most other Tasmanian Cenozoic basalts with similar SiO_2 contents, they are characterised by high alkalis (Na_2O and K_2O), total iron, TiO_2 and P_2O_5, and low MgO and CaO.

On a total-alkali silica plot (Figure 10) of Le Maitre (2002) five of the analyses plot in the trachybasalt field (S_1) and, as they are relatively sodic (Na_2O % > K_2O % +2), they classify as hawaiites in the total alkali-silica IUGS classification for volcanic rocks. The other sample (G408825) marginally qualifies as a mugearite. However, SiO_2 in this sample and G408837, both of which contain secondary chalcedony in amygdales, is higher than in the other four samples.

All samples plot in the alkalic field, well above the empirical boundary between tholeiitic and alkalic basalts of Macdonald and Katsura (1964), and five plot well above the alternative boundary of Irvine and Baragar (1971).
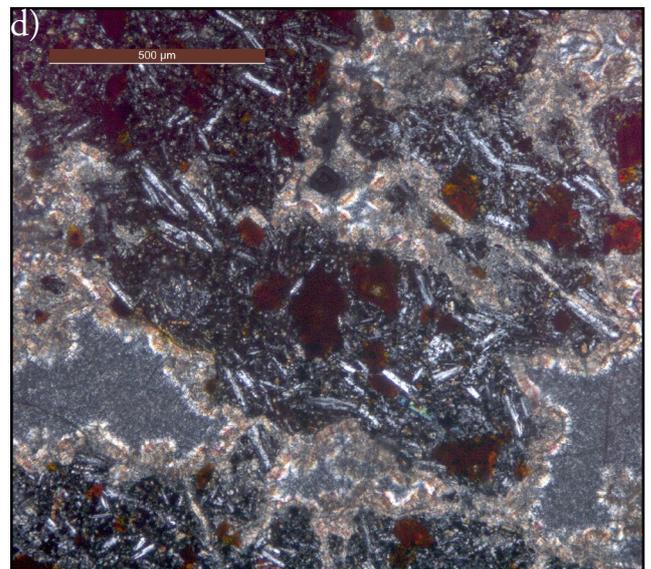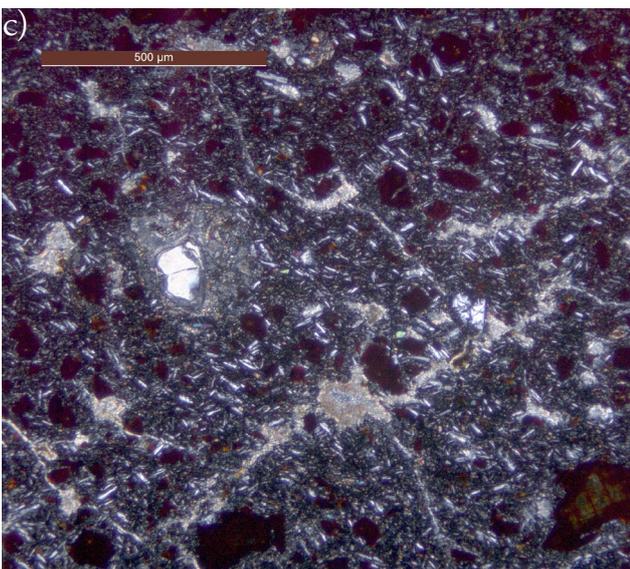
Figure 7. a) Vesicular basalt with patchy to evenly dispersed vesicles and xenoliths indicated with arrow (FOV ~20 cm) indicated by white arrow. b) Compact basalt with vesicular texture. c) Photomicrograph of vesicular basalt with iddingsite replaced dark brown-green olivine phenocrysts in fine grained groundmass of tabular plagioclase and blocky clinopyroxene (crossed polarised light), and d) Photomicrograph under cross-polarised transmitted light showing red, finely porphyritic, iddingsite altered olivine crystals in fine-grained altered groundmass containing plagioclase and clinopyroxene micro-phenocrysts, with vesicles partly filled with secondary clay minerals.

Figure 8. a) Olivine basalt with arcuate to lenticular, irregular shaped ovoid to tapered vesicles or cuspate-vesicular texture. b) Cuspate-vesicular texture with dolerite xenolith (indicated with red arrow) texture and close up view of cuspate texture (see inset where vesicles are traced). c) Highly vesicular, siliceous buchite xenolith, FOV ~140 mm. d) Photomicrograph of red, finely porphyritic, iddingsite altered olivine crystals in fine grained groundmass of plagioclase and clinopyroxene (cross-polarised transmitted light). e) Red, iddingsite altered olivine crystals, in a plagioclase and clinopyroxene groundmass with chalcedony filled ovoid vesicle (v) as indicated (photographed under cross-polarised light).
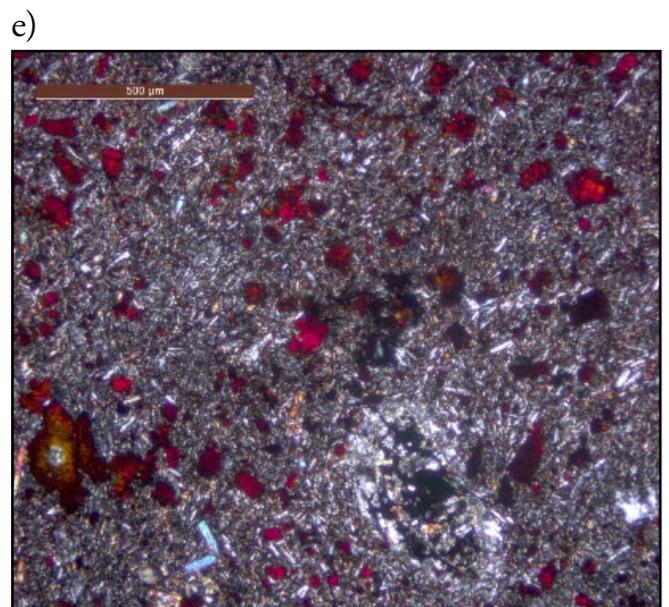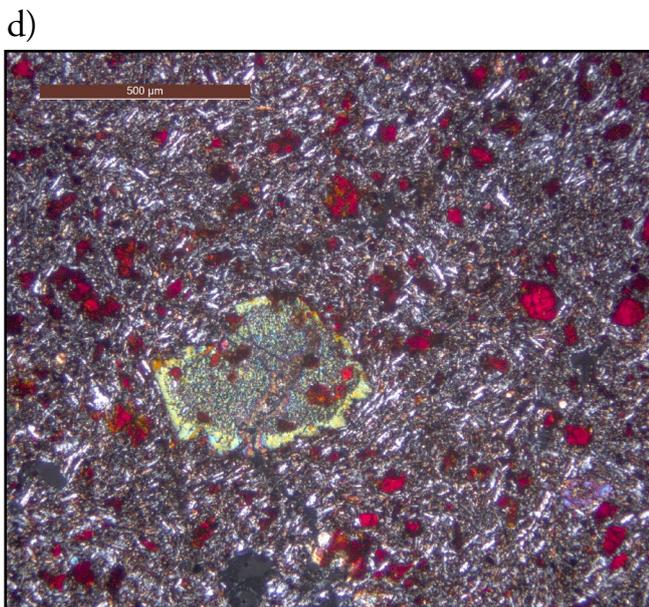
Figure 9. Geochemical plots of Skillion Hill basalt samples (red circles) and SE alkaline group volcanic rocks, showing their alkaline chemistry in relation to the broad subdivisions of Tasmanian Cenozoic basalts.
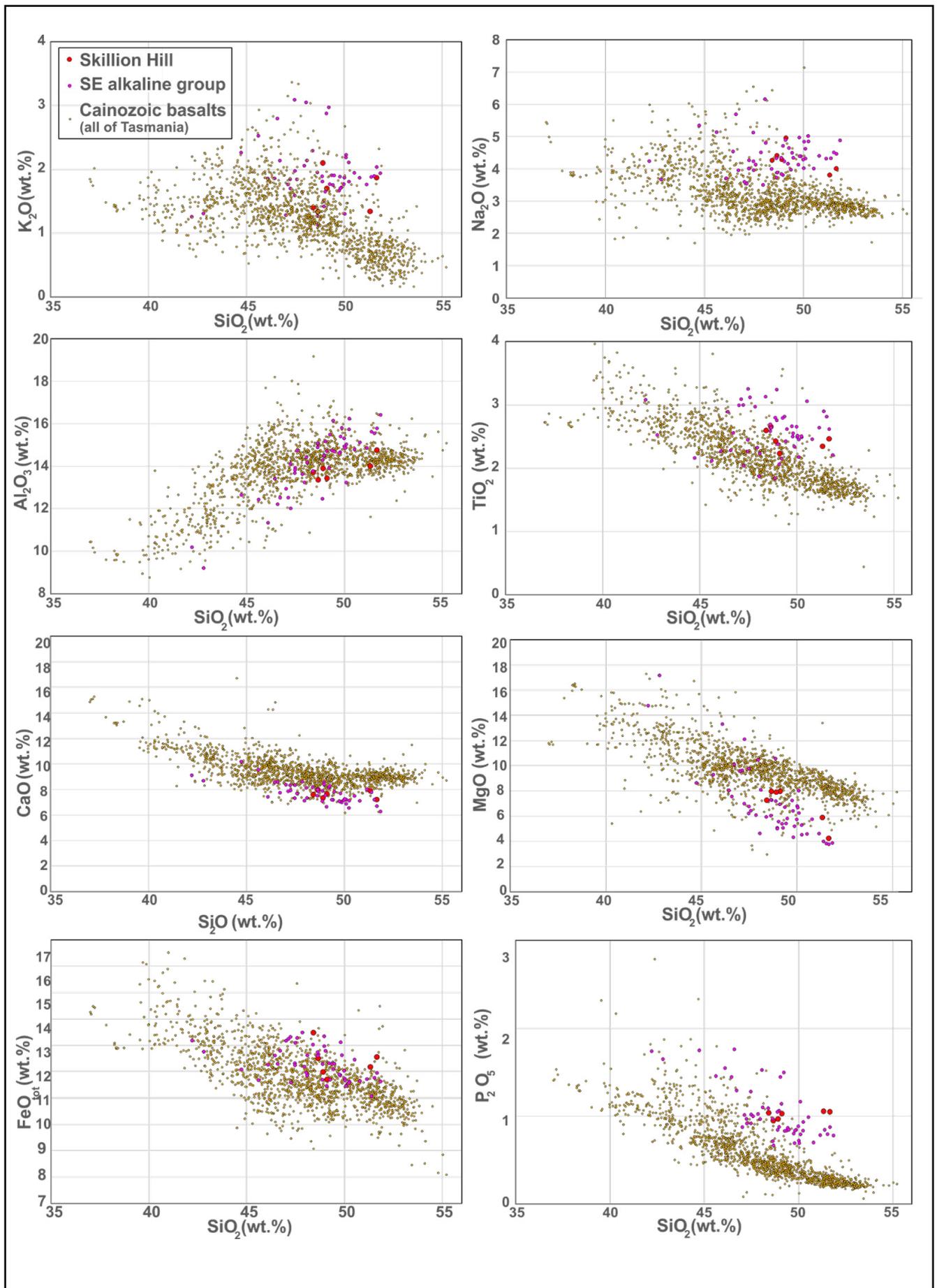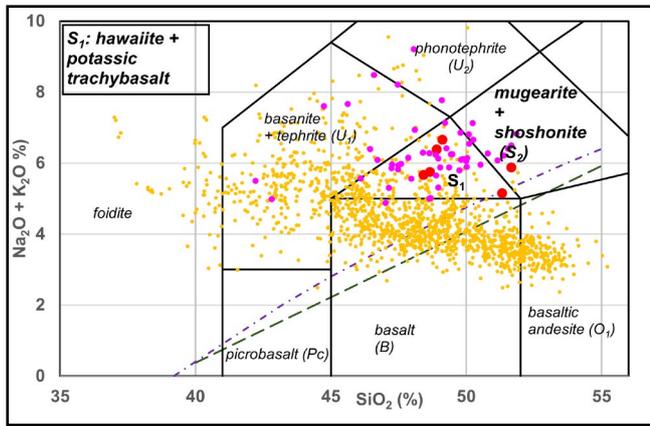
17

Figure 10. SiO$_2$ vs. Na$_2$O+K$_2$O (after Le Maitre (2002)) for the Skillion Hill samples (red), SE alkaline group volcanic rocks and Cenozoic volcanic rocks in Tasmania more broadly.

CIPW norms (after Cross et al., 1902) were calculated at Fe$_2$O$_3$/FeO = 0.2. The norms range from moderately nepheline-normative to moderately hypersthene-normative, but a distinctive feature is the relatively sodic normative plagioclase (An 23.9 to 33.4). In the normative classification (Everard et al., 2014; modified from Johnson and Duggan, 1989) they are variously mugearites, nepheline mugearites, sodic hawaiites and saturated hawaiites.

The most appropriate petrological classification for the lavas at Skillion Hill is probably hawaiite, although in some respects they approach the composition of a mugearite.

The Skillion Hill lavas area also characterised by high levels, relative to other Tasmanian Cenozoic basalts, of incompatible trace elements such as Sr (950-1165 ppm), Zr (365- 490 ppm), Nb (59 -78 ppm), Ba (530 – 705 ppm), light rare earth elements (LREE) and P. This reflects strong fractionation, probably of an alkalic parental magma derived from a low degree partial melt, already relatively elevated in these elements. The strongly compatible elements Ni (310-584 ppm) and Cr (223-269 ppm) are, however, also relatively high for basalts with this relatively low Mg#. This may be due to contamination with mantle xenoliths and their disaggregated debris, which are observed petrographically.

The Skillion Hill rocks belong to a distinctive group of basaltic rocks, common south and east of Hobart but rare elsewhere in Tasmania, comprising fractionated, sodic hawaiites, mugearites and their more undersaturated equivalents. This group was identified petrographically by Edwards (1950), and characterised petrologically by Sutherland (1976, 1985) as the "Southern Hobart Group" or the "alkaline association". It also comprises volcanic centres and associated lavas east of Hobart at Droughty Hill, Acton, Sandford, Cambridge, around Sorell (e.g. Iron Creek), Forcett, Wattle Hill, Primrose Sands and on the Tasman Peninsula (Saltwater River, Lime Bay and Black Rock Hill). Localities west of the Derwent estuary include Sandy Bay (Blinking Billy Point), Mt Wellington (southeast of the Pinnacle), Kingston (Pickett Hill), Mar-

gate, Tinderbox and Kaoota. At many of these localities the lavas are highly vesicular or scoriaceous and may be associated with pyroclastics. Little detailed volcanological work has been done but other documented sites with pyroclastics include Margate (Sutherland, 1985), Firthside near Kingston (Sutherland, 1976; von Lichtan, 2000) Sandy Bay (Spry, 1955), Lime Bay (Brill and Hale, 1954; Gulline, 1984) and Acton (Sutherland, 1976).

3.0 DISCUSSION AND INTERPRETATION

3.1 Scoria breccia deposits: a'ā lava lobes, clinker autoclastite, volcanic bombs and resedimented clinker deposits

The Vesicular basalt is gradational into the Monomictic blocky scoria-rich breccia and is interpreted to represent a highly vesicular lava flow with a blocky, highly vesicular autoclastic crust. The scoria-rich deposits (represented by the Monomictic blocky scoria-rich breccia and Polymictic scoria-rich breccia) peripheral to this flow may, at least in part, represent autoclastite breccia facies such as clinker, a term used to describe massive or scoriaceous fragments commonly associated with 'a'ā lava flows (Loock et. al., 2010; Rowland and Walker, 1990).

The larger (>6.5 cm), lenticular to spheroidal or ribbon shaped scoria clasts observed in Fluidal scoria-rich breccia, and parts of the Stratified scoria-rich breccia show distinct morphologies including banded or vesicular, elongate and spindle shaped clasts. These features are consistent with volcanic bombs or spatter and likely formed from a highly to moderately fluid magma (Sumner et al., 2005). Some of the clasts in the Monomictic blocky scoria-rich breccia are boulder-sized scoria clasts with cracked outer surfaces or bread-crust texture characteristic of volcanic bombs that may have solidified in flight similar to those documented elsewhere (Canon-Tapia, 2017; Fujibayashi et. al., 2014).

Fluidal to ropy components in the Monomictic blocky scoria rich breccia, Fluidal scoria-rich breccia, and Stratified scoria-rich breccia, occur above, beneath and within the Cuspate-vesicular basalt. These breccia facies are all poorly sorted, coarse grained, massive and generally monomictic with elongate, vesicular, variably flow banded, and fluidal lenticular or ribbon shaped clasts. The elongated clasts in the Fluidal scoria-rich breccia and Stratified scoria-rich breccia show flow lines and striations with distinct elongate morphologies similar to volcanic bombs. This material is interpreted to represent deformed and flattened spatter, which may have started as completely fluid clasts that agglutinated (or partly agglutinated) on impact during deposition. The crude stratification in the Stratified scoria-rich breccia may be the result of changes in eruption dynamics, such as eruption column height, fragmentation processes or changes in dispersal patterns during the eruption (McPhie et. al., 1993).

18

3.2 Proximal intra-vent feeder dykes and associated volcanic facies

The scarp along the eastern side of Skillion Hill aids in the recognition of several cross-cutting basaltic zones with compositional banding. The cross-cutting basalt is gradational to cross-cutting Monomictic blocky scoria-rich breccia. Both are interpreted to represent feeder dykes. The dykes exhibit fluidal, irregular margins similar to feeder systems documented elsewhere (Geshi et al., 2014) which suggests the brecciation is syn-eruptive with intrusion.

3.3 Cuspate-vesicular basalt: fountain-fed lavas welded spatter or agglutinate

The cuspate-vesicular texture in the basalt along the eastern scarp could represent discontinuous fine-scale curviplanar jointing, devitrification (perlitic fracture), an alteration texture, or the irregular outline of clasts that have coalesced during fire-fountaining. Subaerial lavas are known to have platy jointing or "tiny normal joints", tortoise shell and curviplanar joints (McPhie et al., 1993). Platy joints parallel to flow direction can also occur in the dense interiors of andesitic flows (McPhie et al., 1993). However, the cuspate features enclose vesicles, and appear irregular in form and orientation (i.e. are not generally planar) therefore cannot be used to determine flow direction. If the features represent finely-spaced platy jointing, vesicle growth would have preceded very irregular (non-planar) movement of the basalt.

Perlitic fractures are most commonly found in hydrated silicic glass, but can also occur in volcanics with mafic and intermediate compositions (McPhie et al., 1993). However, the cuspate fractures are not readily visible in thin sections. Rather, the groundmass is fine-grained, inhomogenous and porphyritic, with rare close-spaced microlites and glassy textures.

The alkaline chemistry is suggestive of low viscosity lavas, and may imply that material was emplaced from low eruption column(s), in which heat loss would have been minimal (Thomas and Sparks, 1992). Therefore, if juvenile pyroclasts formed, they could have sintered and flattened together rapidly on contact to form agglutinate resulting in almost coherent rock (Jones et al., 2018). Hot pyroclasts can deform plastically and weld, due to load compaction (Sparks and Wright, 1979; Wright, 1980), and develop textures and structures similar to lavas (McPhie et al., 1993). Studies of agglutinate (Sumner et al., 2005) suggest matrix textures in such deposits resemble the groundmass textures in coherent lava flows, and separate shards may not be discernible (McPhie et al., 1993). Post-eruption bubble expansion and coalescence can overprint original shallow conduit textures in high temperature and low viscosity basaltic eruptions (Jones et. al., 2018). Microscopic observations to support agglutinate textures in the cuspate-vesicular lava at Skillion Hill

remains inconclusive. However, Fluidal and Monomictic blocky scoria-rich breccia occurs above, beneath and within the Cuspate-vesicular basalt. Monomictic blocky scoria-rich breccia contains in-tact volcanic bombs, deposits of angular to Fluidal scoria-rich breccia and is in close association with cross-cutting dyke or basalt feeders, which all signify a close association with a vent-proximal cone. Textures and components are synonymous with rapid deposition, fire fountaining, and suggest Skillion Hill is a credible setting for agglutinate, or annealed spatter formation. Therefore the cuspate vesicles could represent the space between annealed spatter or agglutinate.

3.4 Petrogenesis

Parental magmas to the "alkaline association" of hawaiite/mugearite were probably of alkali olivine basalt or basanitic composition, generated by low to moderate degrees of mantle partial melting. These relatively low volume melts, with initially moderate volatile contents, stagnated within the mantle. At mantle depths the main liquidus or near-liquidus phases were probably olivine and clinopyroxene, with pressure delaying the crystallisation of plagioclase. Slow cooling with olivine-clinopyroxene fractionation led to an increase in volatile content, alkalis and incompatible trace elements, and a decrease in MgO and CaO. The high volatile content may have been a factor in eventually causing fire fountaining and wall failure (as proposed by Sutherland (1976)). Ascent, probably driven by decompression and expansion of volatiles, was rapid enough to allow the entrainment of mantle xenoliths and xenocrysts (as seen at Skillion Hill). On approaching the surface, the expanding magma tore xenoliths of country rock from the conduit wall and was explosively erupted from small vent(s), with generation of vesicular lavas, spatter, scoria and pyroclastics.

4.0 SUMMARY AND CONCLUSIONS

Skillion Hill consists of evolved alkaline basaltic rocks (mostly hawaiite). The various facies associations are interpreted as lava flows with clinker deposits, feeder dykes, spatter, spatter mounds, and probably agglutinates. Eruptions likely involved alternating low viscosity, volatile-poor magma with high effusion rates (to form coalesced spatter and lava flows) and eruptions with high volatile content, alkalis and incompatible trace elements and likely high explosivity (more agglutinated spatter, scoriaceous breccias and some volcanic bombs). Both are consistent with eruptive products formed from fire fountaining. Annealed spatter indicates rapid accumulation, allowing immediate coalescence of hot impacting clasts during the eruption. Crudely stratified facies may suggest an intermittent change in fragmentation, dispersal or eruption column heights during eruptions. The large xenoliths and feeder dykes suggest the deposits examined were likely close to the vent.

5.0 REFERENCES

Banks, M. R. 1965. Geological Map of Hobart 1:63 360, in Smith, E. M., Williams, E., (ed.) *Geological excursions for the Australian and New Zealand Association for the advancement of Science*, Thirty-eighth congress, 16-20th August 1965. Tasmania Department of Mines.

Bottrill, R. S. and Unwin, L. 2018. Mineralogical Analyses, Skillion Hill, Rokeby. Internal *Mineral Resources Tasmania Mineralogical/Petrology Report,* LJN2018-074.

Brill, K. G. and Hale, G. E. 1954. Geological Map of The North-Western end of Tasman Peninsula - a Revision. *Papers And Proceedings of The Royal Society of Tasmania*, 88, 279-284.

Cañón-Tapia, E. 2017. Mechanism of Formation of Volcanic Bombs: Insights From A Pilot Study Of Anisotropy Of Magnetic Susceptibility And Preliminary Assessment of Analytical Models. *Bulletin of Volcanology*, 79. Https://Doi.Org/10.1007/S00445-017-1136-6.

Calver, C. R. and Latinovic, M. (Compilers) 2002. Digital Geological Atlas 1:25 000 Scale Series. Sheet 5224. *Taroona*. Mineral Resources Tasmania.

Crawford, A. J., Lanyon, R., Elmes, M. and Eggins, S. 1997. Geochemistry and Significance of Basaltic rocks dredged from the South Tasman Rise and adjacent seamounts, *Australian Journal of Earth Sciences,* 44, 621-632.

Cross, W., Iddings, J. P., Pirsson, L. V., Washington, Henry, S. 1902. A quantitative chemico-mineralogical classification and nomenclature of igneous rocks, *The Journal of Geology,* 10/6, 555–690.

Edwards, A. B. 1950. The Petrology of The Cenozoic Basaltic Rocks Of Tasmania. *Proceedings Of The Royal Society Of Victoria,* 62, 97-120.

Everard, J., Baille, P. W., Beyer, E. E., Doyle, R. B., O'reilly, S. Y. and Zhang, M. 2014. Palaeogene–Neogene Basaltic Volcanism. In Corbett, K. D., Quilty, P. G. and Calver, C. R. (Eds.), *Geological Evolution Of Tasmania* (463–494). Geological Society Of Australia (Tasmania Division).

Forsyth, S. M. and Clarke, M. J. (Compilers) 1999. Digital Geological Atlas 1:25 000 Scale Series. Sheet 5225. *Hobart*. Mineral Resources Tasmania.

Fox, J. M., Mcphie, J., Carey, R. J. and Jourdan, F. 2023. Revised Stratigraphy And First Geochronology of The Miocene Submarine Volcanic Succession At Kennaook/Cape Grim, Northwestern Tasmania, *Australian Journal of Earth Sciences,* 70, 510-534.

Fujibayashi, N., Asakura, K., Hattori, T. and Allen, S. 2014. Pillow Lava And Spasmodic Submarine Fire Fountaining In The Middle Miocene Marginal Basin, Sado Island, Japan, *Island Arc*, 23, 344-364.

Geshi, N., and Neri, M. 2014. Dynamic Feeder Dyke Systems In Basaltic Volcanoes: The Exceptional Example Of The 1809 Etna Eruption (Italy), *Frontiers in Earth Science*, 2, https://doi.org/10.3389/feart.2014.00013.

Green, D. C. 1961. The Geology of The South Arm-Sandford Area, *Papers And Proceedings Of The Royal Society Of Tasmania,* 95, 177-199.

Gulline, A. B. 1984. Geological Survey Explanatory Report. Geological Atlas 1:50 000 Series. Sheet 83 (8412s). *Sorell*. Tasmania Department of Mines.

Irvine, T. N. and Baragar, W. R. A. 1971. A guide to the chemical classification of common volcanic rocks. *Canadian Journal of Earth Sciences*, 8, 523-548.

Johnson, R. W. 1989. *Intraplate Volcanism In Eastern Australia And New Zealand*. Cambridge University Press.

Johnson, R. W. and Duggan, M. B. 1989. Rock Classification And Analytical Data Bases. In: Johnson, R. W. (Ed.). *Intraplate Volcanism In Eastern Australia And New Zealand*, 12-13. Cambridge University Press.

Jones, T. J., Houghton, B. F., Llewellin, E. W., Parcheta, C. E. and Holtgen L. 2018. Spatter Matters – Distinguishing Primary (Eruptive) And Secondary (Non-Eruptive) Spatter Deposits, *Scientific Reports,* 8/9179.

Leaman, D. E. 1972. Geological Atlas 1:50 000 Series, Sheet 82 (8312s). *Hobart*. Tasmania Department Of Mines.

Le Maitre, R. W. (ed.) 2002. *A Classification of Igneous Rocks And Glossary Of Terms*, 2nd Edition. Cambridge University Press, 236.

Loock, S., Van Wyk De Vries, B. and Hénot, J-M. 2010. Clinker Formation In Basaltic And Trachybasaltic Lava Flows, *Bulletin Of Volcanology*, 72.

Macdonald, G. A. and Katsura T. 1964. Chemical Composition of Hawaiian Lavas. *Journal Of Petrology*, 5, 82-133.

McPhie, J., Doyle, M. and Allen, R. 1993. *Volcanic Textures: A Guide To The Interpretation Of Textures In Volcanic Rocks*. Centre For Ore Deposit And Exploration Studies, University Of Tasmania, Hobart.

Rowland, K. R. and Walker, G. P. L. 1990. Pahoehoe And Aa In Hawaii: Volumetric Flow Rate Controls The Lava Structure, *Bulletin of Volcanology*, 52, 615–628.

Sumner, J. M., Blake, S., Matela, R. J. and Wolff J. A. 2005. Spatter, *Journal of Volcanology And Geothermal Research*, 142, 49–65.

Sutherland, F. L. 1971. The question of late Cainozoic uplifts in Tasmania, *Search*, 2, 430-431.

Sutherland, F. L. 1976. Cenozoic Volcanic Rocks; In Leaman D. E. Geological Survey Explanatory Report. Sheet 82 (8312s). *Hobart*. Tasmania Department of Mines.

Sutherland, F. L. 1977. Cenozoic Volcanic Rocks; In Leaman D. E. (Ed.) Geological Survey Explanatory Report. Sheet 75 (8312n). *Brighton*. Tasmania Department of Mines.

Sutherland, F. L. 1985. Cenozoic Volcanic Rocks; In Farmer, N. Geological Survey Explanatory Report. Sheet 88 (8311n). *Kingborough*. Tasmania Department of Mines.

Sutherland, F. L. and Wellman, P. 1986. Potassium-Argon ages of Tertiary Volcanic Rocks, Tasmania, *Papers And Proceedings Of The Royal Society Of Tasmania,* 120, 77-86.

Sutherland, F. L., Graham, I. T., Everard, J. L., Forsyth, S. M. and Zwingmann H. 2004. Cenozoic Basalts, Tasmania: Landscapes, Exposures, Ages, Petrography, Geochemistry, Entrainments And Petrogenesis, *Geological Society Of Australia Field Guide A5*, 17th Australian Geological Convention, Hobart, February 2004.

Sparks, R. and Wright, J. 1979. Welded air fall tuffs, *Geological Society of America Bulletin*, Special Paper 180, 155–166.

Spry, A. H. 1955. The Tertiary Volcanic Rocks Of Lower Sandy Bay, Hobart, *Papers And Proceedings Of The Royal Society Of Tasmania,* 89, 153-168.

Thomas, R. M. E. and Sparks, R. S. J. 1992. Cooling of Tephra during Fallout from Eruption Columns, *Bulletin of Volcanology*, 54, 542-553. http://dx.doi.org/10.1007/BF00569939.

von Lichtan, I. J. 2000. *Characteristics And Origin of Proximal Volcanic Breccias In Hydrothermal Tertiary Basalt Centres, In South-East Tasmania*. Bsc Hons Thesis, University Of Tasmania, Hobart (Unpubl.).

Wright, J. 1980. Stratigraphy and geology of the welded airfall tuffs of Pantelleria, Italy, *Geologische Rundschau*, 69, 263–291.

Zwingmann, H., Sutherland, F. L., Graham, I., Forsyth, S. M., Everard, J. L. and Wartho, J.-A. 2004. New K-Ar And Ar-Ar Ages For Ne Tasmanian Basalts: Implications For Volcanic Evolution Following Tasman Rifting. *Geological Society of Australia Abstracts,* 73, 141.

APPENDIX 1

Additional petrographic notes

Sample R010110 (HBJ33)

A sample (HBJ33/R010110) was collected from the northern flow at the junction of Pass Road and Goodwins Road. In thin section it consists of very sparse, mostly anhedral to subhedral phenocrysts of olivine and rare clinopyroxene in a fine-grained fluidal intergranular groundmass.

The olivine phenocrysts are up to 2.5 mm across with a crudely subhedral outline and ragged, slightly embayed margins, but more commonly ≤1 mm and anhedral. At least some of the phenocrysts may be enocrysts. They are about 20-30 % altered to dark brown iddingsite around their margins and along internal fractures.

Rare euhedral microphenocrysts (≤ 500 µm) of clinopyroxene have pale pink titaniferous rims, and may have colourless cores. There are also rare digested xenocrysts, up to 2.5 mm long, possibly former orthopyroxene of lherzolitic origin, which has reacted to an aggregate of small euhedral prisms (~200-100 x 40-10 µm) of pale yellow-green clinopyroxene, minor dark red-brown biotite (?) and brown-stained secondary carbonate (Figure 10).

The groundmass consists of small crudely aligned plagioclase laths (typically 200 – 100 µm long), intergranular equant to shortly prismatic granules of clinopyroxene, abundant equant opaque grains (typically 10 – 40 µm across) and patches of pale greenish-brown to dark brown alteration products.
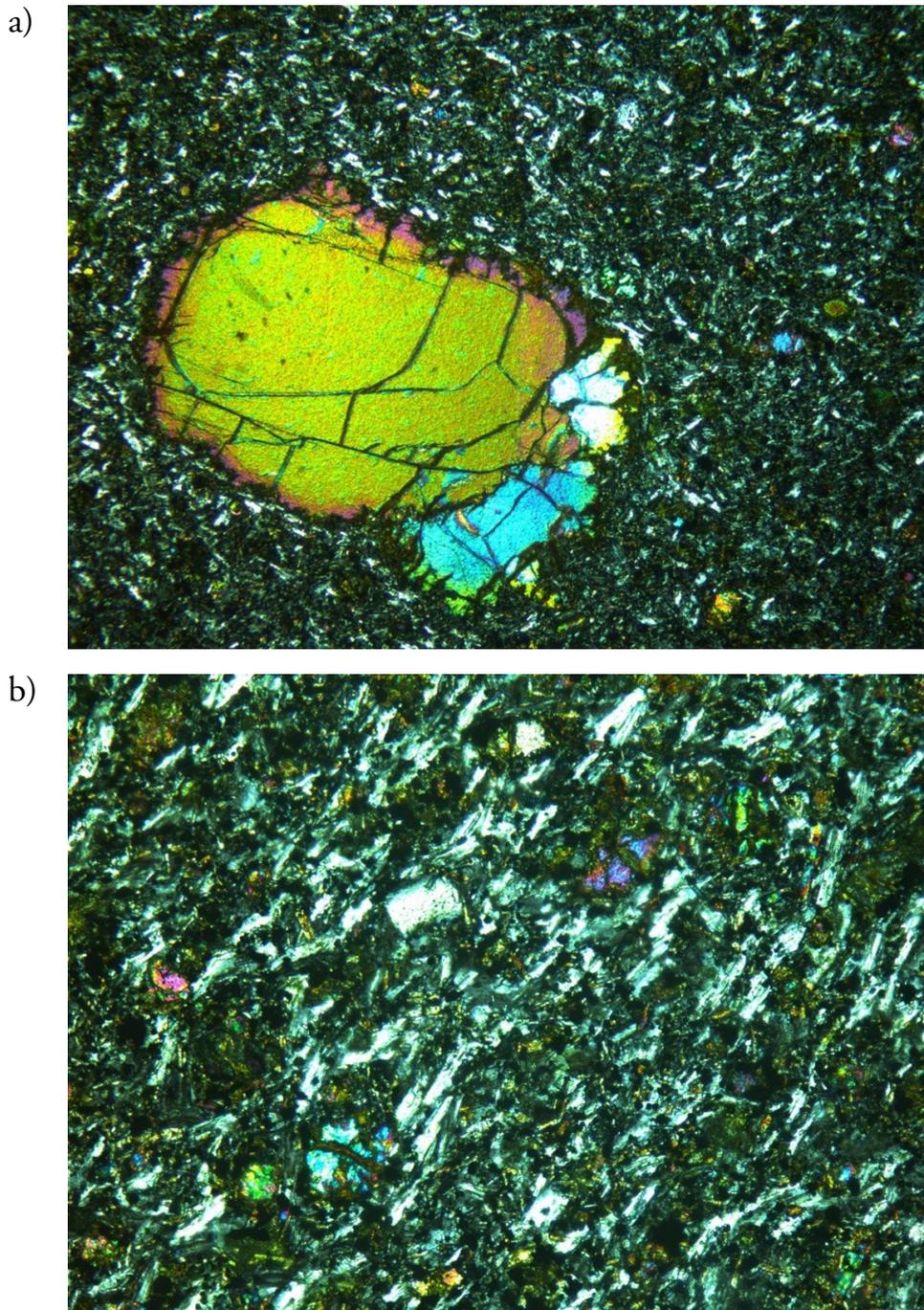
a)

b)

Figure 10. Sample HBJ33 under cross-polarised light showing a) Olivine phenocryst (2.5 mm across) with dark brown iddingsite around margins and along internal fractures. b) Groundmass with crudely aligned plagioclase laths (typically 200 – 100 µm long).

Sample R010109 (HBJ32)

This sample was collected from near the junction of Rokeby Road and Pass Road, immediately northeast of Skillion Hill, and is probably from a scoria breccia facies.

The thin section consists of fine-grained, altered basalt with few vesicles, passing into a zone of very amygdaloidal basalt enclosing a small (~15 mm) xenolith of Jurassic dolerite.

The enclosing basalt contains abundant (~15-20%) but small (≤400 μm, mostly ~150 μm) euhedral microphenocrysts of olivine, almost entirely replaced by bright brownish-red iddingsite with a rare unaltered cores. The groundmass consists of densely packed, unoriented pla-gioclase laths (~50 – 100 μm long), smaller granules and prisms of clinopyroxene and very abundant equant opaque grains (5 – 50 μm across) in an indeterminate low birefringence mesostasis. A few anhedral probable xenocrysts are present, including a corroded clinopyroxene grain and altered olivine with pale yellow cores and dark brown iddingsite rims.

Amygdales near the margin of the basalt are filled with clay minerals and relatively coarse-grained, well-crystallised nepheline and possible zeolites. The dolerite xenolith is of a relatively coarse-grained (~4-5 mm) feldspathic variety, consisting mainly of interlocking to ophitically intergrown plagioclase and augite.

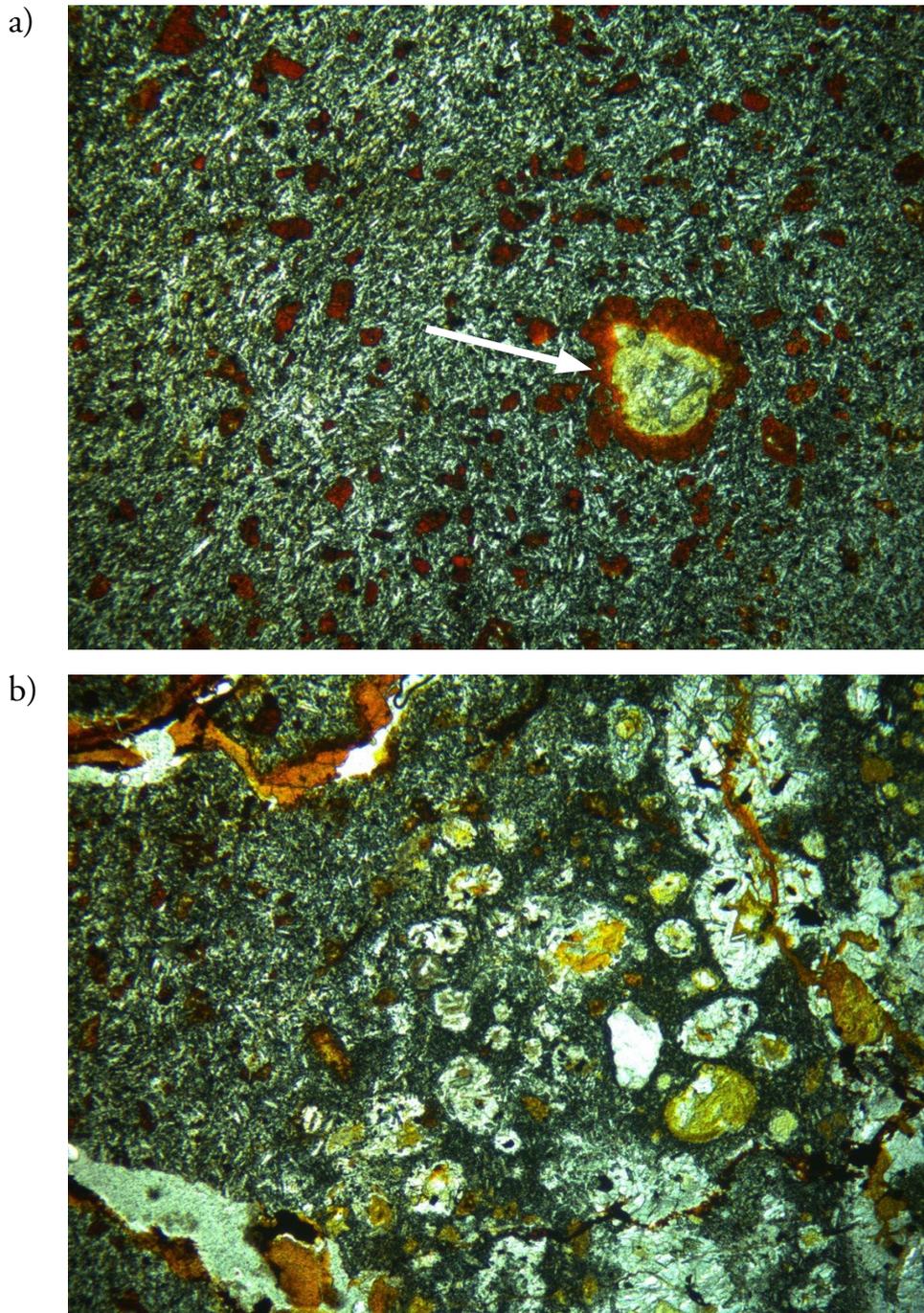Figure 11. Sample HBJ32 under normal light showing a) euhedral microphenocrysts of olivine, with outer margin of bright brownish-red iddingsite and unaltered core (arrow), and b) amygdaloidal zone near the margin of the basalt filled with clay minerals and relatively coarse-grained, well-crystallised nepheline and possible zeolites.

APPENDIX 2

Whole rock major and trace element analyses from the Skillion Hill area

Table X. Whole rock analyses and CIPW norms

MRT Reg No	C112290	C112292	G408825	G408837	R010110	-
Field/other No	-	-	-	-	HBJ33	ABE6-1
mEgda94	534889	534901	534749	534738	~534980	~534600
mNgda94	5251058	5250900	5251244	5251164	~5251850	~5251700
SiO2	48.20	47.68	49.71	48.60	47.58	46.64
TiO2	2.19	2.60	2.37	2.22	2.36	2.50
Al2O3	13.19	13.10	14.21	13.27	13.53	13.22
Fe2O3	*12.77	*13.62	*13.43	*12.82	4.21	9.81
FeO	nd	nd	nd	nd	7.88	4.16
MnO	0.17	0.16	0.16	0.12	0.16	0.19
MgO	7.83	7.82	4.09	5.59	7.69	7.01
CaO	7.52	7.81	6.94	7.48	7.14	7.33
Na2O	4.87	4.33	3.86	3.61	4.17	4.11
K2O	1.67	1.31	1.80	1.27	2.04	1.35
P2O5	1.01	0.93	1.01	1.00	0.94	1.00
H2O+	nd	nd	nd	nd	1.67	0.52
H2O-	nd	nd	nd	nd	nd	2.14
CO2	nd	nd	nd	nd	0.05	nd
C	<0.1	<0.1	<0.1	<0.1	nd	nd
SO3	nd	nd	nd	nd	0.04	nd
LOI	0.28	0.52	2.08	3.76	0.84	nd
TOTAL	**100.10**	**100.24**	**100.07**	**100.14**	**99.45**	**99.98**
FeOtot	11.49	12.26	12.08	11.54	11.66	12.99
Mg#(0.20)	58.90	57.30	41.59	50.48	58.12	53.17

(* total iron as Fe2O3)

trace elements (parts per million)

S	<200	1200	500	1900	nd	
Sc	16	17	15	14	14	
V	134	169	115	151	130	
Cr	249	269	223	265	230	
Co	75	74	63	52	38	
Ni	370	377	504	584	310	
Cu	51	55	90	98	62	
Zn	147	141	174	148	155	
Ga	25	24	27	25	26	
As	8	7	6	6	<20	
Rb	14	18	13	11	24	
Sr	1165	947	1190	1150	1150	
Y	31	31	33	32	32	
Zr	438	365	468	418	490	
Nb	76	59	77	74	78	
Mo	7	6	3	6	6	
Sn	<2	<2	<2	<2	<9	
Sb	<1	<1	<1	<1	nd	
Ba	697	606	705	700	530	
La	59	56	68	63	63	
Ce	132	111	141	122	145	
Nd	55	56	68	57	69	
W	nd	nd	nd	nd	<10	
Pb	9	7	11	8	<10	
Bi	2	<1	2	1	<5	
Th	11	9	11	11	13	
U	3	2	3	2	<10	

CIPW norms calculated at Fe2O3/FeO = 0.20

or	10.03	7.88	11.03	7.91	12.38	8.26
ab	28.02	29.93	33.85	32.18	27.29	31.21
an	9.35	12.66	16.72	17.12	12.44	14.12
ne	7.51	3.99	-	-	4.84	2.60
di	17.85	16.83	10.13	12.45	14.35	13.79
hy	-	-	13.99	15.82	-	-
ol	17.71	18.39	4.07	4.61	18.88	19.37
mt	2.87	3.07	3.08	2.99	2.94	3.30
il	4.23	5.03	4.67	4.44	4.60	4.92
ap	2.42	2.23	2.47	2.49	2.28	2.44
total	**100.00**	**100.00**	**100.00**	**100.00**	**100.00**	**100.01**
An mol% plag	23.92	28.51	31.76	33.40	30.05	29.89
Normative classification	nepheline mugearite	mugearite	saturated hawaiite	saturated hawaiite	sodic hawaiite	mugearite
IUGS classification	mugearite	hawaiite	hawaiite	hawaiite	hawaiite	hawaiite

Mineral Resources Tasmania
PO Box 56 Rosny Park
Tasmania Australia 7018
Ph: +61 3 6165 4800

info@mrt.tas.gov.au   www.mrt.tas.gov.au